Supplementary Materials

A stretchable all-nanofiber pressure sensor

Yigen Wu[1], Shuai Dong[1], Xiaojuan Li[2], Liguo Wen[2], Hongwei Shen[2], Mengjiao Li[2], Xin Liu[1], Yang Zhang[1], Guolong Zeng[1], Jianyi Zheng[1,*], Dezhi Wu[1,*]

[1]Pen-Tung Sah Institute of Micro-Nano Science and Technology, Xiamen University, Xiamen 361005, China.
[2]Beijing Smart-chip Microelectronics Technology Co., Ltd, Beijing 102211, China.

*Corresponding Author: zjy@xmu.edu.cn (J. Zheng), wdz@xmu.ehu.cn (D. Wu)

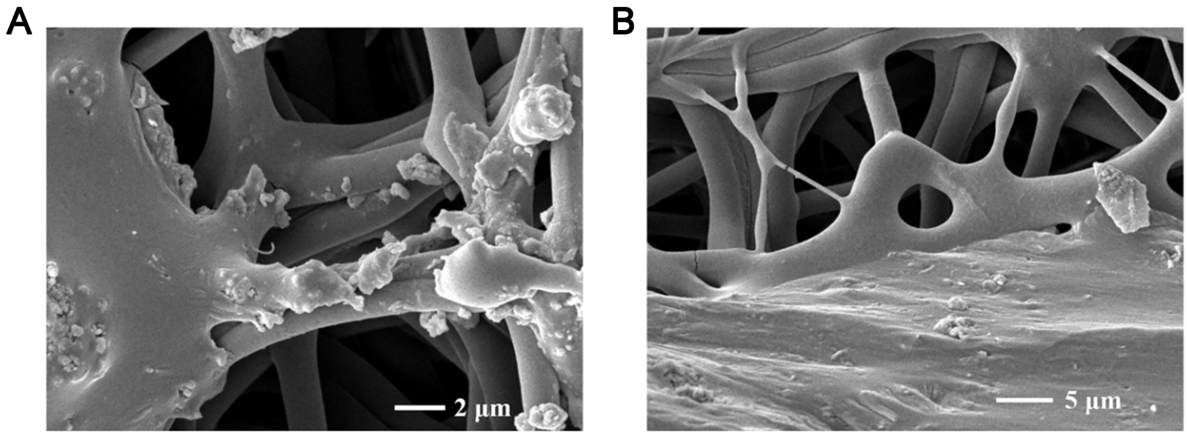

Supplementary Figure 1. The SEM images of interfacial interaction between liquid metal of (A) pristine TPU nanofibers and (B) composited GO/TPU nanofibers.

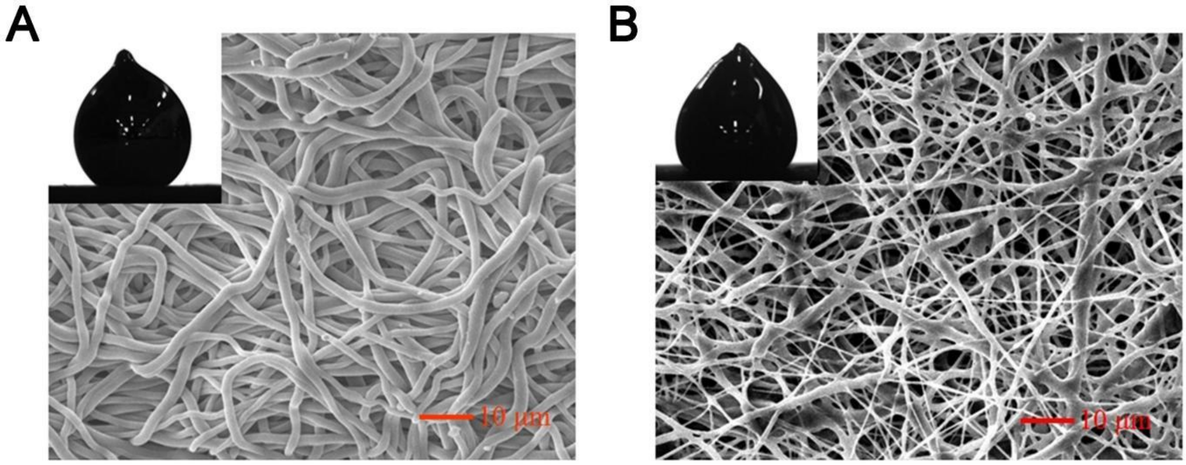

Supplementary Figure 2. SEM images of (A) TPU and (B) GO/TPU nanofibers membrane. Inset is a photograph showing the contact angle of liquid metal to corresponding substrate.

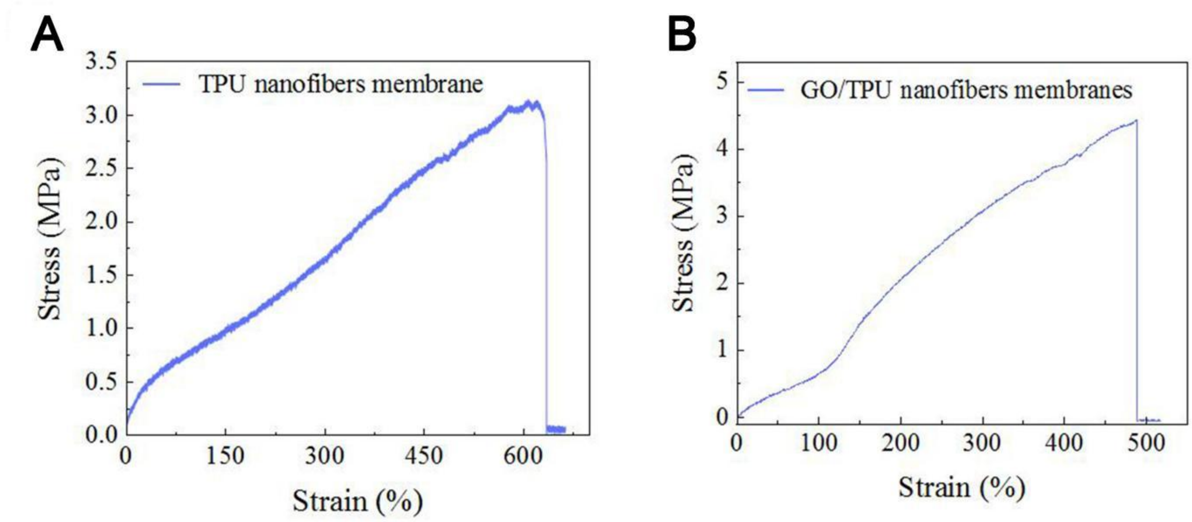

Supplementary Figure 3. Stress-strain curves of (A) pure TPU nanofiber membrane and (B) GO/TPU nanofibers membrane.

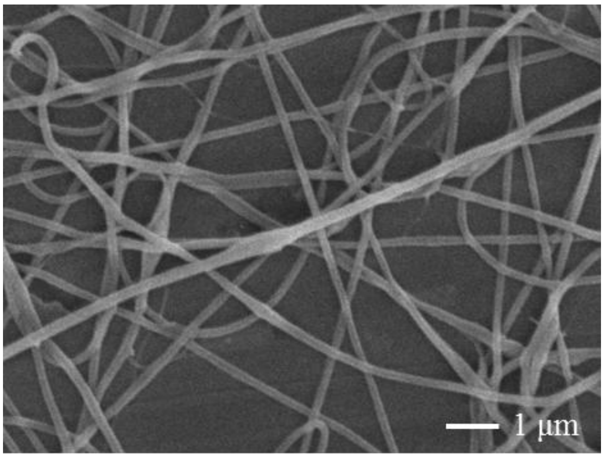

Supplementary Figure 4. SEM images of the pure PVDF-HFP nanofibers.

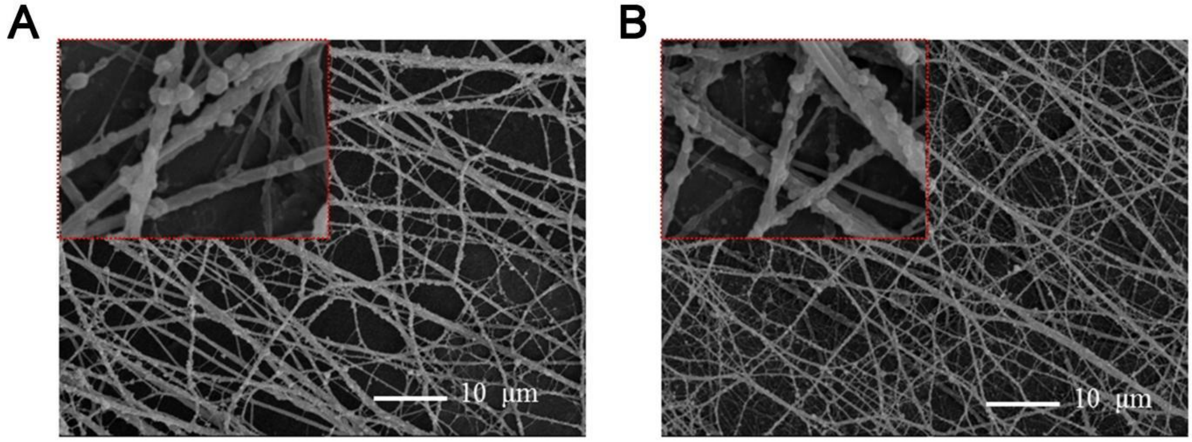

Supplementary Figure 5. SEM images of the iontronic PVDF-HFP/[EMIM][TFSI] nanofibers with a weight ration of (A) 1:2 and (B) 1:1.

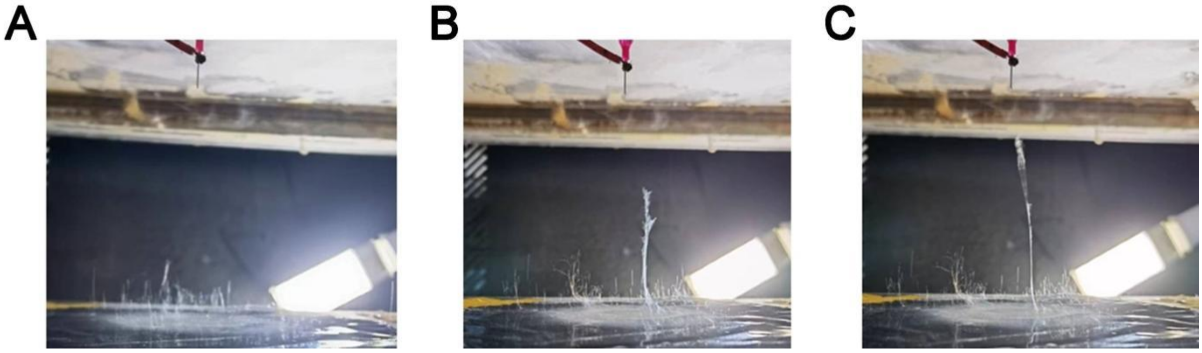

Supplementary Figure 6. Electrospinning process of the PVDF-HFP/[EMIM][TFSI] iontronic nanofibers with iontronic liquid weight rate of 2:1.

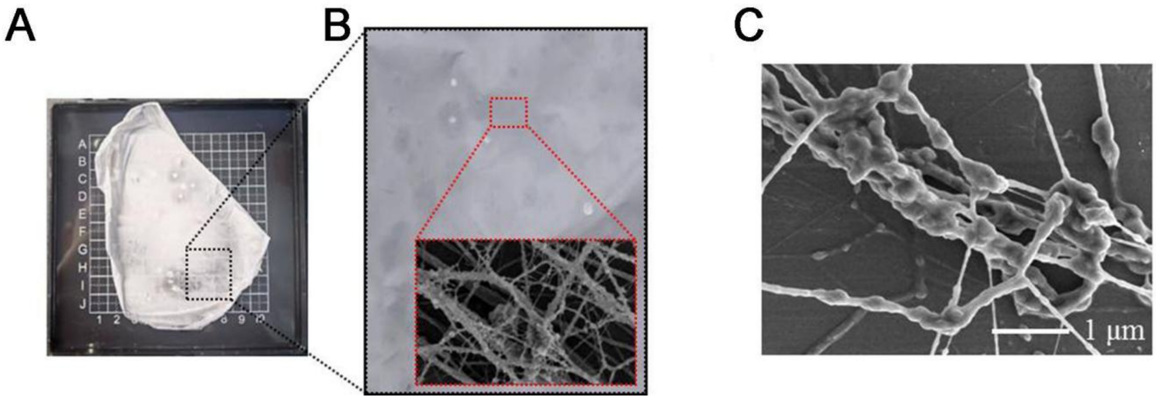

Supplementary Figure 7. Photographs and SEM images of the iontronic PVDF-HFP/[EMIM][TFSI] nanofibers with a weight ration of 1:2.

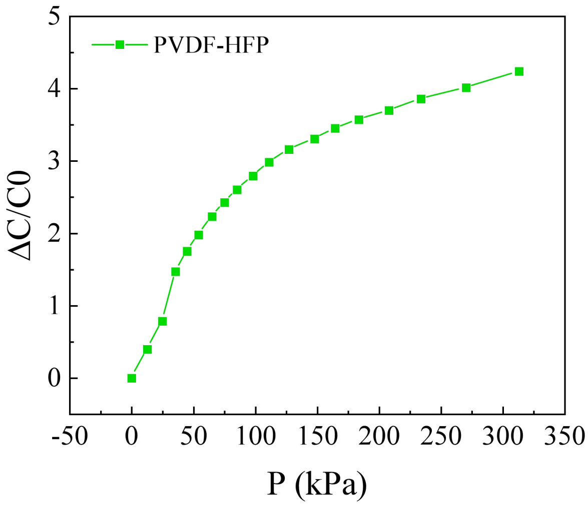

Supplementary Figure 8. Response-pressure curves of the sensor with PVDF-HFP nanofibers membrane as the dielectric layer.

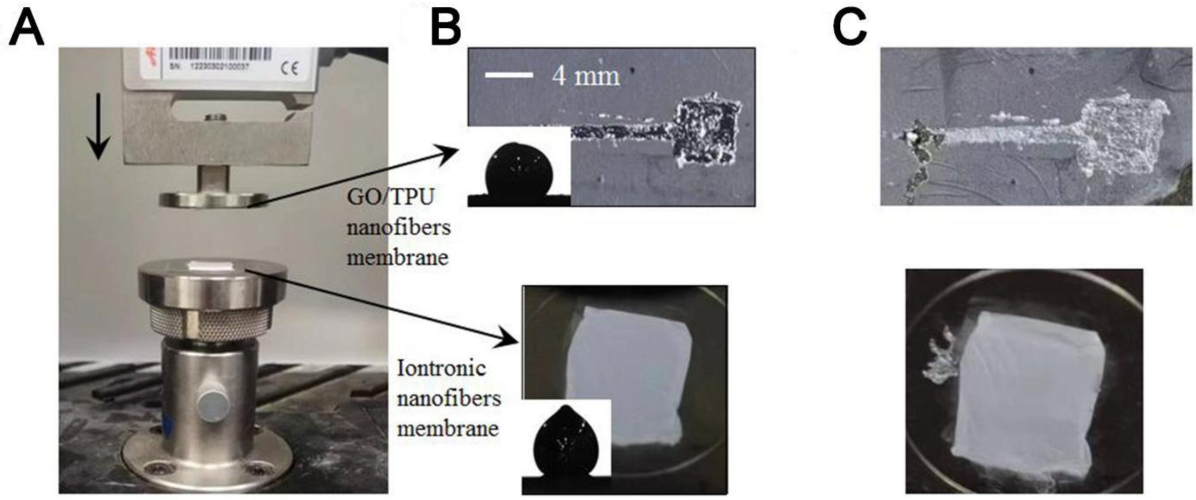

Supplementary Figure 9. The selective adhesion test of liquid metal to GO/TPU nanofibers membrane and iontronic nanofibers membrane. (A) The experimental setup of liquid metal electrode structural stability test based on selective adhesion. The images of liquid metal electrode structure (B) before and (C) after 5000 compression cycles.

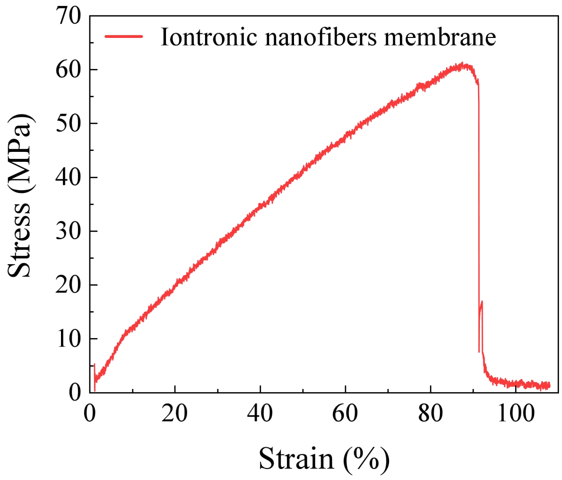

Supplementary Figure 10. Stress-strain curves of the iontrinic nanofibers membrane.

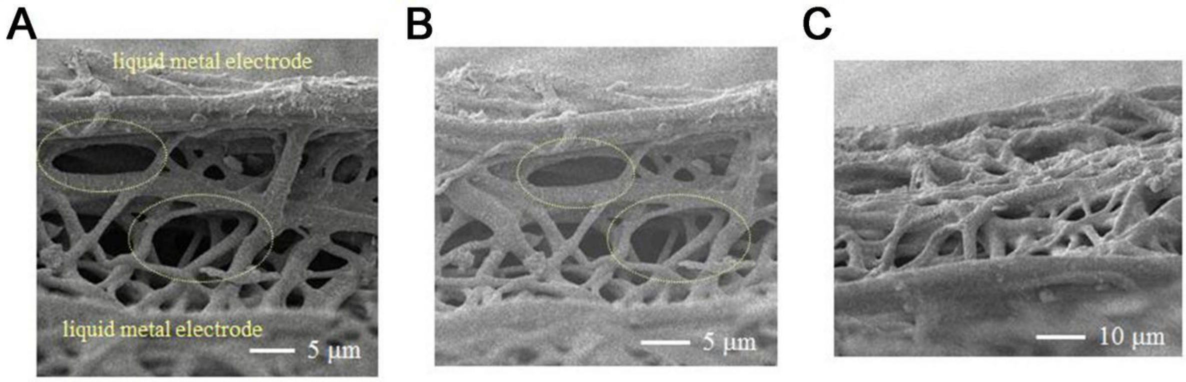

Supplementary Figure 11. Cross-sectional view SEM image of the sensor under (A) initial state, (B) compression state with 10 kPa applied pressure and (C) compression state with 300 kPa applied pressure, showing that the porosity of the ionic nanofibers membrane decreases with increasing of applied pressure.

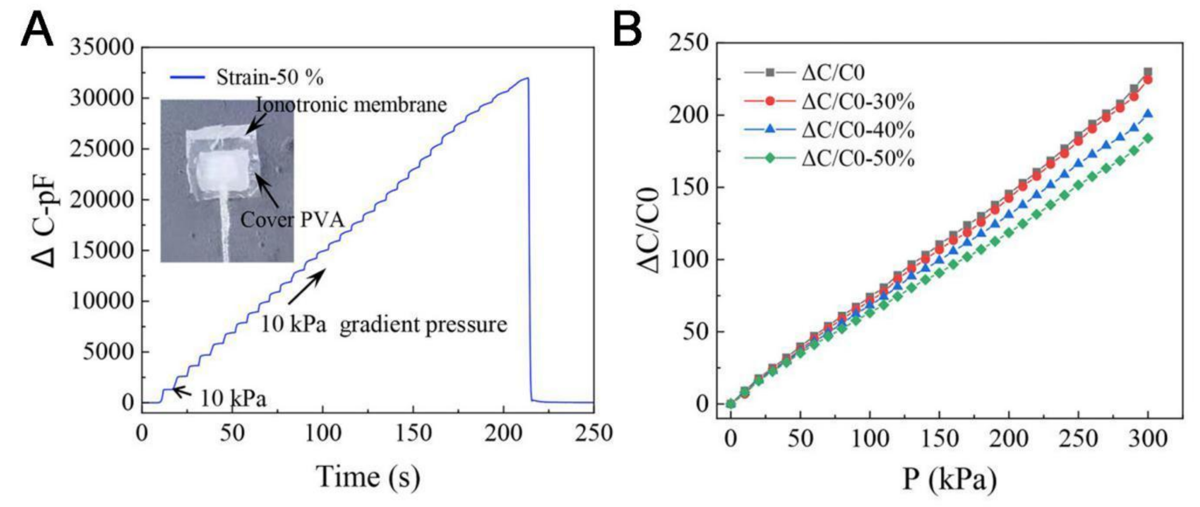

Supplementary Figure 12. The approach of improving the stretchability of the SNIPS. (A) The capacitance output of the SNIPS varies with the gradient external pressure under 50% stretching condition. (B) Sensitivity curves of the SNIPS under different stretching deformation.

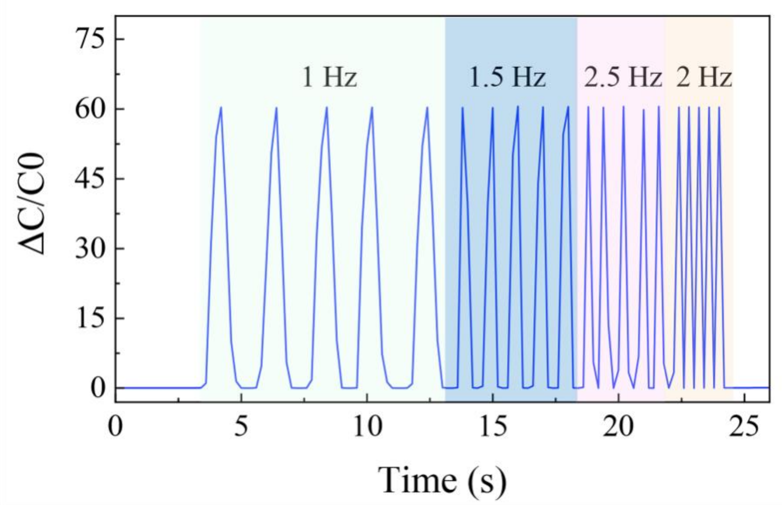

Supplementary Figure 13. The corresponding normalized capacitance changes of the SNIPS to different external 100 kPa pressure with diverse frequencies under the condition of 50% stretching.

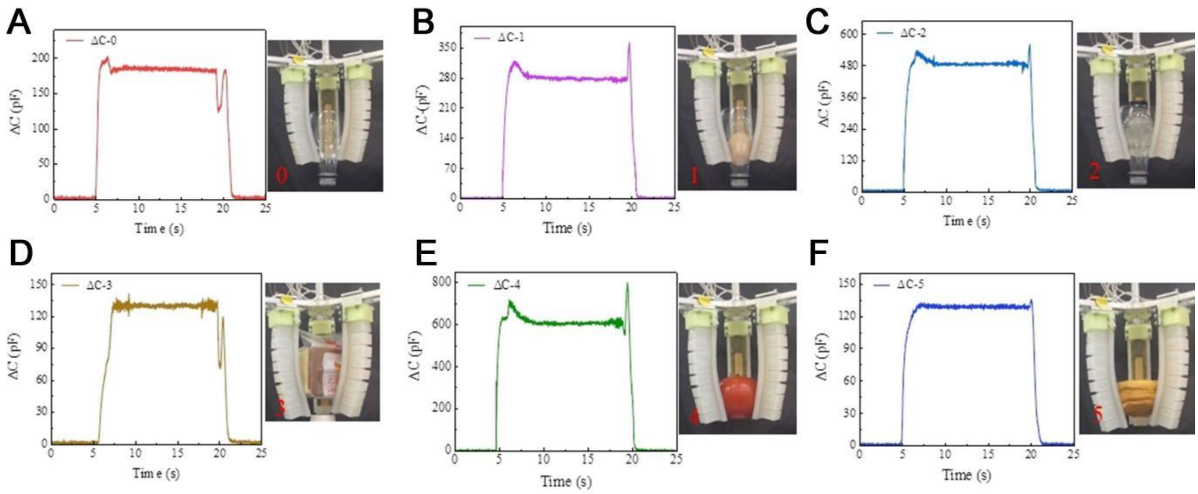

Supplementary Figure 14. The photograph of grasping different objects and its corresponding capacitance changes during the gripping process. (A) Grasped object 0 of an empty bottle container about 15 g. (B) Grasped object 1 of an empty bottle container loaded with an egg about 65 g. (C) Grasped object 2 of an empty bottle container loaded with a bottle of water glue about 205 g. (D) Grasped object 3 of an empty bottle container loaded with a bag of bread about 75 g. (E) Grasped object 4 of an empty bottle container loaded with a tomato about 175 g. (F) Grasped object 5 of an empty bottle container loaded with a loaf of bread about 55 g.

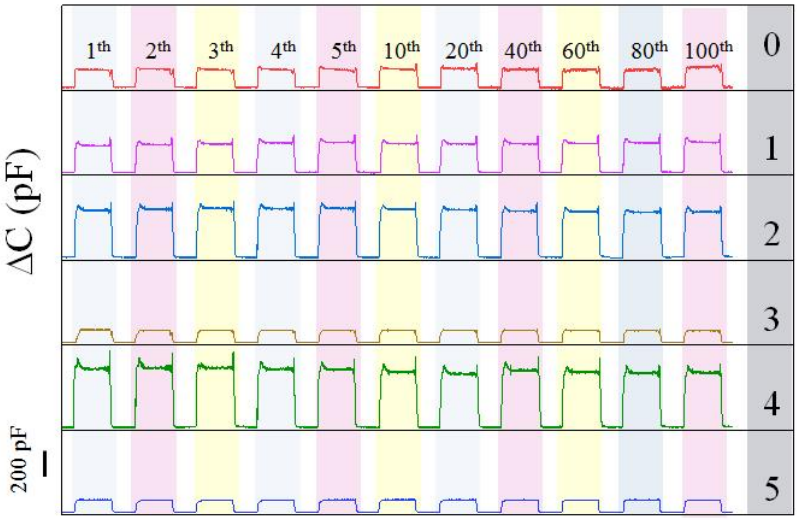

Supplementary Figure 15. Output capacitance changes of objects 0-5 with grasping 100 times.

Supplementary Table 1. Comparison of our SNIPS with previously reported flexible capacitive pressure sensor

Ref.	**Fabrication method**	**Structure**	**Sensitivity**	**Stability & Stretchability**
1	Mouding and assembly	Dielectric: double interlocked layered microcone structure Electrode: Au film	8035.1 kPa^{-1}	NA.
2	Electrospinning and assembly	Dielectric: hydrogel Electrode: PEDOT:PSS	12 kPa^{-1}	NA.
3	Silicon moulding and layer assembly	Dielectric: microstructured PDMS Electrode: ITO film	0.55 kPa^{-1}	15000 bending cycles & no stretching
4	Mouding and assembly	quasi-homogeneous composition with interlinked interfaces	0.15 kPa^{-1}	15000 shearing cycles & no stretching
5	Mold from calathea zebrine and assembly	Dielectric: microstructured ionic gel Electrode: AgNWs	54.31 kPa^{-1}	5400 compressing cycles & no stretching
6	Mold from sandpaper and assembly	Dielectric: intrafillable microstructured Electrode: Au film	220 kPa^{-1}	5000 compressing cycles and 2000 bending cycles & no stretching
7	electrospinning and assembly	Dielectric: ionic nanofibers membrane Electrode: graphene	217.5 kPa^{-1}	20000 compressing cycles & no stretching
8	electrospinning and assembly	Dielectric: ionic nanofibers membrane Electrode: AgNWs	6.21 kPa^{-1}	6000 compressing cycles & no stretching
9	electrospinning and assembly	Dielectric: ionic nanofibers membrane Electrode: multiwall	0.97 kPa^{-1}	NA.

		carbon nanotube		
10	Wet spinning	Electrode: electrospun reinforced conductive fibers	NA.	NA.
11	Electrospinning and ultrasonication	N/A	NA.	100000 stretcing cycles
This work	Electrospinning	Dielectric: ionic nanofibers membrane Electrode: liquid metal	1.08 kPa^{-1}	5000 compressing cycles and 5000 stretching cycles & 50 % stretching strain

References

1. Niu HS, Li H, Gao S, Li Y, Wei X, Chen YK, Yue WJ, Zhou WJ, Shen GZ. Perception-to-cognition tactile sensing based on artificial-intelligence-motivated human full-skin bionic electronic skin. Adv. Mater. 2022; 34, 2202622: 1-11. DOI: https://doi.org/10.1002/adma.202202622

2. Guo YJ, Yin FF, Li Y, Shen GZ, Lee JC. Incorporating wireless strategies to wearable devices enabled by a photocurable hydrogel for monitoring pressure information. Adv. Mater. 2023; 202300855: 1-11. DOI: https://doi.org/10.1002/adma.202300855

3. Mannsfeld SCB, Tee BCK, Barman S, Reese C, Bao ZN, et al. Highly sensitive flexible pressure sensors with microstructured rubber dielectric layers. Nature mater. 2010; 9, 859-864. DOI: https://doi.org/10.1038/nmat2834

4. Zhang Y, Yang JL, Hou XY, Zhang ZY, Guo CF, et al. Highly stable flexible pressure sensors with a quasi-homogeneous composition and interlinked interfaces. Nat. Commun. 2022; 13, 1317. DOI: https://doi.org/10.1038/s41467-022-29093-y

5. Qiu ZG, Wan YB, Zhou WH, Yang JY, Wang H, Guo CF, et al. Ionic skin with biomimetic dielectric layer template from calathea zebrine leaf. Adv. Funct. Mater. 2018; 28, 1802343. DOI: https://doi.org/10.1002/adfm.201802343

6. Bai NN, Wang L, Wang Q, Zhao XH, Guo CF, et al. Graded intrafillable architecture-based iontronic pressure sensor with ultra-broad-range high sensitivity. Nat. Commun. 2020; 11,209. DOI: https://doi.org/10.1038/s41467-019-14054-9

7. Lin XZ, Xue H, Li F, Mei HX, Zhao HR, Zhang T. All-nanofibrous ionic capacitive pressure sensor for wearable applications. ACS Appl. Mater. Interfaces 2022; 14, 31385-31395. DOI: https://doi.org/10.1021/acsami.2c01806

8. Cui XH, Chen JW, Wu W, Liu Y, Li HD, Xu ZG, Zhu YT. Flexible and breathable all-nanofiber iontronic pressure sensors with ultraviolet shielding and antibacterial performances for wearable electronics. Nano energy 2022; 95, 107022. DOI: https://doi.org/10.1016/j.nanoen.2022.107022

9. Mahanty B, Ghosh SK, Maity K, Roy K, Shakar S, Mandal D. All-fiber pyro- and piezo-electric nanogenerator for loT based self-powered health-care monitoring. Mater. Adv. 2021; 2, 4370. DOI: 10.1039/d1ma00131k

10. Veeramuthu L, Cho CJ, Zhou BX, Kuo CC, Lee WY, et al. Muscle fibers inspired electrospun nanostructures reinforced conductive fibers for smart wearable optoelectronics and energy generators. Nano energy 2022; 101, 107592. DOI: https://doi.org/10.1016/j.nanoen.2022.107592

11. Tian ZH, Qin WJ, Wang YL, Li XX, Gu CS, Chen JJ, Yang M, Feng L, Chen JX, Qiao HY, Yin SG. Ultra-stable strain/ humidity dual-functional flexible wearable sensor based on brush-like AgNPs@CNTs@TPU heterogeneous structure. Colloids and surfaces A: physicochemical and engineering aspects 2022; 670, 131398. DOI: https://doi.org/10.1016/j.colsurfa.2023.131398